Research of Pattern Formation, edited by R. Takaki, pp. 549–564.

The State of the Art of Medical 3-D Image Processing

Shigeki YOKOI and Takami YASUDA

Department of Information Engineering, School of Engineering, Nagoya University, Nagoya 464-01, Japan

Abstract. Three dimensional (3-D) information in medical images has a great deal of potential to be used not only for diagnostic but also therapeutic purposes. Several 3-D visualization techniques have been reported to render human internal organs as clearly as possible. It is now possible to interactively manipulate these 3-D images on a graphic terminal just as a surgeon would do during a surgery.

This article examines the current developments for both visualization and manipulation of medical 3-D images such as X-ray CT in order to be used for actual clinical application.

1. Introduction

Image processing has quite an important role in order to effectively utilize digital images which have been generated and acquired in various kind of industrial fields. In the medical area, digital recorded medical images have been often used for diagnosis and medical treatment. CT (Computed tomography) image is one of the most useful for clinical medicine, since without any invasions the human body can be visualized as cross sectional images, and a set of CT images acquired along one direction has three dimensional (3-D) anatomical informations. Using a computer, these 3-D quantity can be reconstructed and displayed on the screen, since CT images record physical property such as x-ray absorption in the form of digital data. Required processes for this purpose in the computer generally include "modeling", "projection", "rendering" and "manipulation" after extracting the region of interest automatically or manually.

These image processings have been studied based on digital image processings and computer graphics, and general fundamental schemes have been surveyed by Yokoi *et al.* (1982), Toriwaki (1986), Udupa (1988), and the most recent works including surgical simulation have been introduced by Yasuda (1989). There are many clinical applications of 3-D medical imaging; for example, surgical planning, radiation therapeutic planning, and anatomical diagnosis. In this article, the current developments for modeling, projection, rendering and manipulation are described.

2. Modeling

In order to reconstruct 3-D shape from a set of sectional images, three typical methods have been proposed such as wire-flame method, triangulation and voxel method.

2.1 Wire-flame method

In this method, contours extracted from all of the CT images represent the 3-D shape by stacking them. Contours are taken out automatically or manually depending on the features of CT value in the interesting region. One has to manually specify the borders of the region if the CT property in the region is not clearly different from the one in the surrounding area. After a set of points on an actual border are extracted, they are smoothly connected by interpolated curves such as spline (Foley *et al.*, 1982; Kaneda, 1981). Stacked boards obtained by sweeping borders upward and downward shown in Fig. 1 are also able to represent the 3-D shape (Yasuda *et al.*, 1984). It is called border sweeping method.

All of these methods roughly express the 3-D shape though, it cannot be used for precise observation.

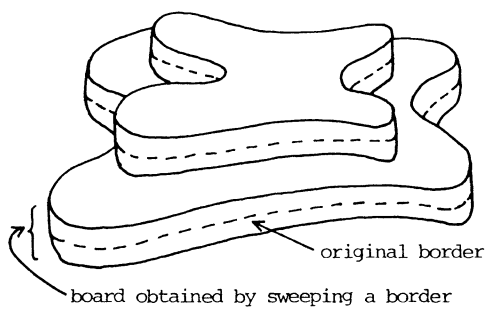

Fig. 1. Border sweeping method.

2.2 Triangulation

3-D surface is obtained by constructing triangular patches from sampled contour points on adjacent two CT slices based on a cost function (Fig. 2). Keppel *et al.* (1975) used trigonal pyramid volume, and Fuchs *et al.* (1977) used triangular area as the cost function. Christiansen *et al.* (1977) simplified the cost calculation to use edge length in a triangle which connects adjacent slices. Although above methods represent the 3-D shape smoothly, they cannot be applied to the cases in which contour shapes between the slices are largely changed or the number of contours are quite different. For these cases, Lin *et al.* (1988) has recently reported a method to use virtual contours distorted by a kind of force field between slices in order to connect contours smoothly.

Human body has several parts whose shapes are cylindrical such as an arm or spherical as head. Therefore, it is reasonable to express these shapes in cylindrical coordinate system or polar coordinate system. A skull surface constructed by contour points in cylindrical coordinate system is shown in Fig. 3 (Yasuda *et al.*, 1986). This is effectively applied to predict post-operative face or

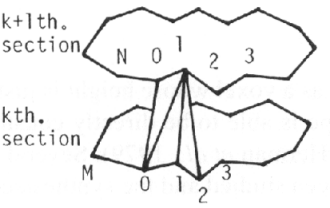

Fig. 2. Triangulation.

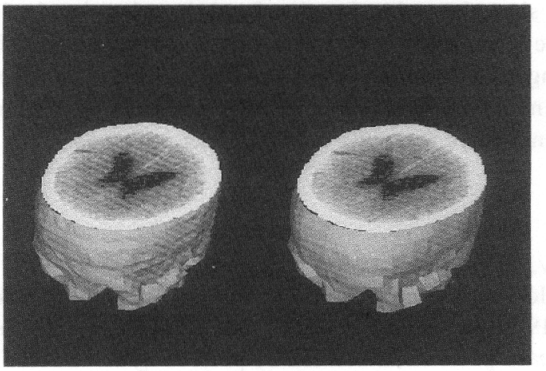

Fig. 3. Skull surface made by triangular patches described in cylindrical coordinate system (stereo images).

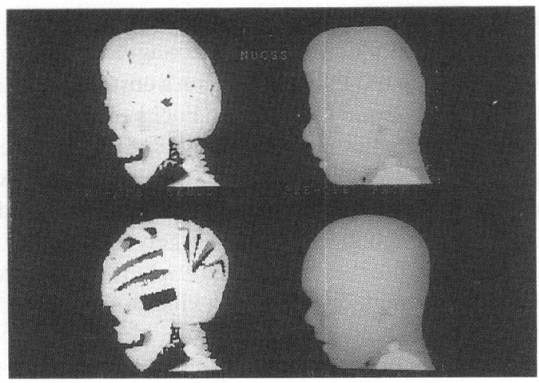

Fig. 4. Prediction of the post-operative face. Pre-operative skull and face (up) the simulated skull and face (down).

head shape after bone grafts in craniofacial surgical planning in Fig. 4 (Yasuda *et al.*, 1990).

2.3 Voxel method

Considering a pixel as a voxel whose height is just the same as the distance between slices, 3-D shape is able to be directly constructed by voxels without generating any patches (Herman *et al.*, 1979). Several rendering techniques for the voxel method have been studied and the synthesized image quality has been improved. Although voxel method is simple, it can be applied to any complex shapes if and only if the region of interest has been extracted. On the other hand, the image quality would be decreased, if image resolution was insufficient, that is, the voxel size was too big. Lorensen *et al.* (1987) has proposed a method to obtain precise shape by estimating tiny facets based on local relations of voxel position. There are 256 kinds of facet combinations due to voxel value (0 or 1). However, using topological equivalence, the combination can be reduced to 14. The rendering method by patches is effective implemented on a work station with a graphic engine which is rapidly able to render polygons.

3. Projection

Generally, hidden surface removal is necessary in order to generate a comprehensible image. Depth(Z) buffer method is often used for this purpose (Foley *et al.*, 1982; Sutherland *et al.*, 1974). Hidden surface removal process is performed at each pixel on the screen by projecting the nearest face of a voxel whose distance to the screen (Z-value) is the shortest among other voxels along the projection line. Projection is usually time consuming, since many voxels

construct a 3-D shape. Therefore, rapid projection schemes have been required. Artzy (1979) has indicated that it is no need to project all six faces of the nearest voxel, since only three faces are always visible from viewing direction.

Back-to-front algorithm utilizes the order of the voxel projection to avoid Z buffer comparison. In this scheme, the farther a voxel exists from the viewer, the faster projected (Herman *et al.*, 1981). By the same group, another approach called front-to-back algorithm is proposed, which the nearer voxel is projected faster and if a screen pixel has been already fulfilled by a projected voxel, no more voxels can be projected on it.

Frieder *et al.* (1985) have pointed out that if the edge length of the voxel is the same as the pixel size on the screen or less than that, no holes would appear on the displayed image even if only the center point of the voxel is projected. They also use a look-up-table for rapid projection. Projection equation from a voxel V(I, J, K) to a screen coordinate (X, Y, Z) is generally described as Eq. (1).

$$\begin{pmatrix} X \\ Y \\ Z \end{pmatrix} = \begin{pmatrix} L_1 & L_2 & L_3 \\ M_1 & M_2 & M_3 \\ N_1 & N_2 & N_3 \end{pmatrix} \begin{pmatrix} I \\ J \\ K \end{pmatrix} + \begin{pmatrix} I_0 \\ J_0 \\ K_0 \end{pmatrix} \tag{1}$$

where 3×3 matrix is a transformation matrix, and translation on the display plane is represented by the term (I_0, J_0, K_0). Three products L_3K, M_3K, and N_3K are calculated once for each slice, since K is fixed for a slice. Other six products L_1I M_1I, N_1I, L_2J, M_2J and N_2J are stored in six one-dimensional arrays for all I and J, and read from them using I or J as an index. Yokoi *et al.* (1987) have developed a much faster projection method which reduces the number of the product, and needs no array. Assuming L_3K, M_3K, and N_3K have been already found for the K-th slice, these values on the next slice are calculated as follows.

$$L_3(K + dK) = L_3K + L_3dK \tag{2}$$

$$M_3(K + dK) = M_3K + M_3dK \tag{3}$$

$$N_3(K + dK) = N_3K + N_3dK \tag{4}$$

where dK is the length of the voxel in K direction. Thus there is no need of multiplication and only one addition can produce the desired values, once L_3K, M_3K, and N_3K are found. A similar approach is used for I and J directions. This procedure then can calculate all elements of the transformation matrix only by addition operations, after the initial values and the increment amounts have already been found by nine multiplies. Frieder's method, on the other hand, needs

$9 \times N$ multiplications for the original image whose size is $N \times N \times N$. N^3 multiplications might be necessary, if no tables are prepared. Based on this feature, Trivedi (1985) used run length expression in order to reduce memory occupancy and to make projection process faster.

4. Rendering

Since 3-D shape constructed by a set of voxels has bumpy shapes on it, several rendering algorithms have been developed to reduce this defect as much as possible.

4.1 Diffuse model

This method uses diffuse reflection model to render the face of voxels. This brightness calculation was first introduced by Herman *et al.* (1979) who originally proposed a voxel based 3-D display scheme. The brightness is given by Eq. (5).

$$I(\theta) = a\{\cos(\theta / n)\}^p \tag{5}$$

where θ is the angle between lighting direction and normal vector on the object surface, a is a constant value related to the maximum intensity of the display device, n and p are parameters concerning smoothness of generated images, respectively. We used $n = 2, p = 0.6$ for instance. Two dimensional filtering is also used in order to eliminate small bumpy noises on the surface.

4.2 Depth coding

The brightness is decided by the distance d between the voxel and the image plane (Vannier *et al.*, 1983).

$$I(d) = a(R - d) \tag{6}$$

where R is the longest distance from image plane to the position where a voxel might exist. This scheme was often used since the voxel shape itself could not be visualized so that the object surface looked smoothly. However, since the details on the surface is also disappeared, it is now used for perspective effect in other brightness calculations.

4.3 Gradient shading

This shading method calculates brightness to estimate the normal vector on the object surface from Z buffer (Gordon, 1985). Z buffer records the distance (Z value) from viewing point to the surface. The object surface is now described as follows.

$$z = Z(x, y) \tag{7}$$

In this case, normal vector at an arbitrary point on the surface is given in Eq. (8).

$$(\partial z / \partial x, \partial z / \partial y, -1) \tag{8}$$

Assuming that δ_f be the subtraction from the present pixel to right one, and δ_b be the subtraction from the present one to left one, $\partial z/\partial x$ could be described as follows.

$$\frac{\partial z}{\partial x} \simeq \frac{W(|\delta_b|)\delta_b + W(|\delta_f|)\delta_f}{W(|\delta_b|) + W(|\delta_f|)} \tag{9}$$

$$W(\delta) = \begin{cases} 1, & \text{if } \delta \le a, \\ 0, & \text{if } \delta \ge b, \\ (1-\varepsilon)/2 + (1-\varepsilon)/2\cos(\delta - a)\pi/(b-a), & \text{otherwise} \end{cases} \tag{10}$$

where $a = 2.0$, $b = 5.0$, $\varepsilon = 10^{-5}$. The same process can be applied to y component. The weight function W is now often used in order to reduce the bumpy shape of the voxel and to express the essential shape of the object. 2-D filtering techniques to smooth Z buffer may be effective to eliminate small bumpy noise without

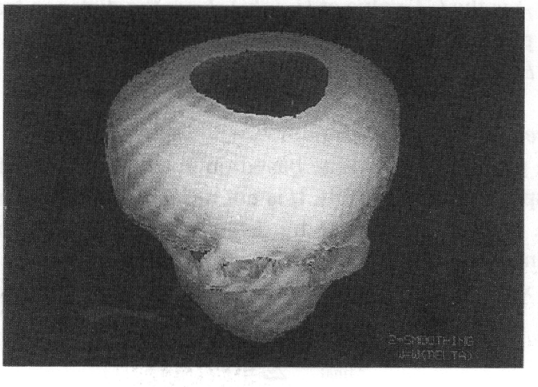

Fig. 5. Skull rendered by gradient shading with variable weight filter.

losing essential shape of the object. The variable weight filter has been proposed for this purpose, and compared with the other three kinds of smoothing filters (Yokoi *et al.*, 1987). An example rendered by gradient shading with variable weight filter is shown in Fig. 5.

4.4 Normal-based contextual shading

This is a method to estimate the object normal based on the state of neighbor voxels (Chen *et al.*, 1986). Its advantage is that the results are rotationally invariant, that is, the estimated normal vector does not change as the object is rotated.

Let p be the center point of a voxel face which constructs the object surface. Assuming u and v are the vectors which are parallel to the edges of the face, the normal vector w is defined as the cross-product for vectors u and v. There are 9 possible directions for vector u however, the actual number can be reduced to 5. Determination of v is analogous. After all, 25 different orientations of w are possible. One disadvantage of this method is that, for a given surface, 81 possible contexts produce only 25 distinct values of w.

4.5 Gray level gradient shading

In order to estimate the object normal more precisely, CT values can be used instead of binary voxels (Höhne *et al.*, 1986). According to this scheme, the projected intensity would be as follows.

$$I(i,j) = A\cos\frac{-\frac{1}{9}\sum_{m=-1}^{1}\sum_{n=-1}^{1}\{g(i+m,j+1,k_T+n)-g(i+m,j-1,k_T+n)\}}{B} - Ck_T \tag{11}$$

where $g(i, j, k_T)$ is the CT value at (i, j, k_T), k_T is the distance from pixel (i, j) on the projected plane to the voxel whose CT value is more than given threshold value, and A, B, C are used as scaling factors.

4.6 Volume rendering

This is a rendering technique based on a sampled scalar function in three dimensional space (Drevin, 1988). It is not necessary to fit geometric primitives for rendering. Images are formed by directly shading each sample points and projecting them onto the image plane. The brightness at a pixel is given by sample value such as x-ray absorption in x-ray CT and opacity in Eq. (12) (Fig. 6)

$$I_{\text{final}} = \sum_x \xi(x)\cdot I(x) \tag{12}$$

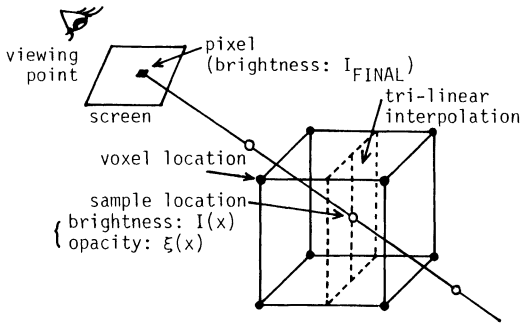

Fig. 6. Volume rendering.

where $I(x)$ and $\xi(x)$ are sample value and opacity at sample point x.

5. Manipulation

After 3-D shapes can be reconstructed from a set of CT images in a computer for precise diagnosis, the next step is to manipulate displayed 3-D images interactively on the screen. This kind of function would help surgeons to make the adequate surgical plan especially for orthopaedic surgery or craniofacial surgery (Ogino *et al.*, 1983; Kurihara *et al.*, 1989). Several researches in this field have been already reported as follows.

(1) 2-D interactive manipulation on a CT image.
(2) Manipulation by fundamental geometric shapes.
(3) 3-D interactive manipulation on a projected image.
(4) Automatic segmentation between two adjacent different bony regions.

5.1 2-D interactive manipulation

In order to remove some parts of the bony region, contours are manually specified on all CT images in a graphic terminal (Bloch *et al.*, 1983). As an application of this kind of process on CT images, Brewster *et al.* (1984) estimates normal shape of the affected part of the skull by using its symmetry on cross sections shown in Fig. 7. It is useful in pre-operative planning for craniofacial surgery.

5.2 Manipulation of fundamental geometric shape

Brewster *et al.* (1984) and Trivedi (1986) proposed a scheme to cut part of the 3-D object by fundamental geometric shapes such as sphere, cube or their combinations. This is performed by binary logical algebra. When an object M is added to an object O, for example, post-operative object O' is described as Eq. (16).

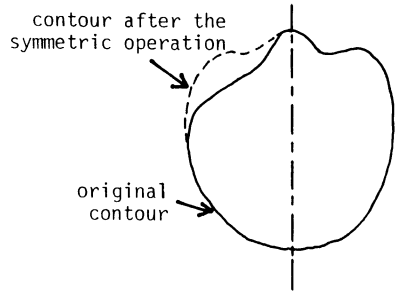

Fig. 7. Estimation of normal shape on a cross section by using symmetry.

$$O' = O \cup M \tag{16}$$

Subtraction is performed in the same manner as Eq. (17) shown in Fig. 8.

$$O' = O \cap \overline{M} \tag{17}$$

The object used here can be also defined by logical algebra such as logical sum of two objects as Eq. (18).

$$M = A \cup B \tag{18}$$

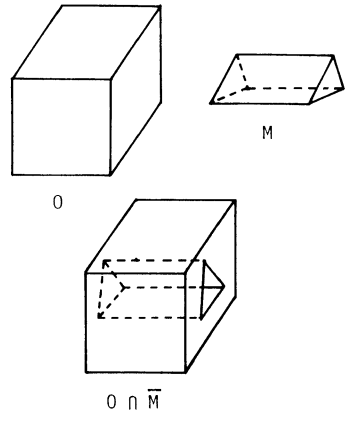

Fig. 8. Manipulation by fundamental geometric shapes.

5.3 3-D Interactive manipulation

The basic principle in this approach is to interact with the object through its depiction in view space. It transforms the user-specified manipulative operation in view space to one in object space as if carrying out the operation in object space. Interactive operation is often restricted to only orthogonal views such as the views obtained when the viewing direction is perpendicular to one of the principal

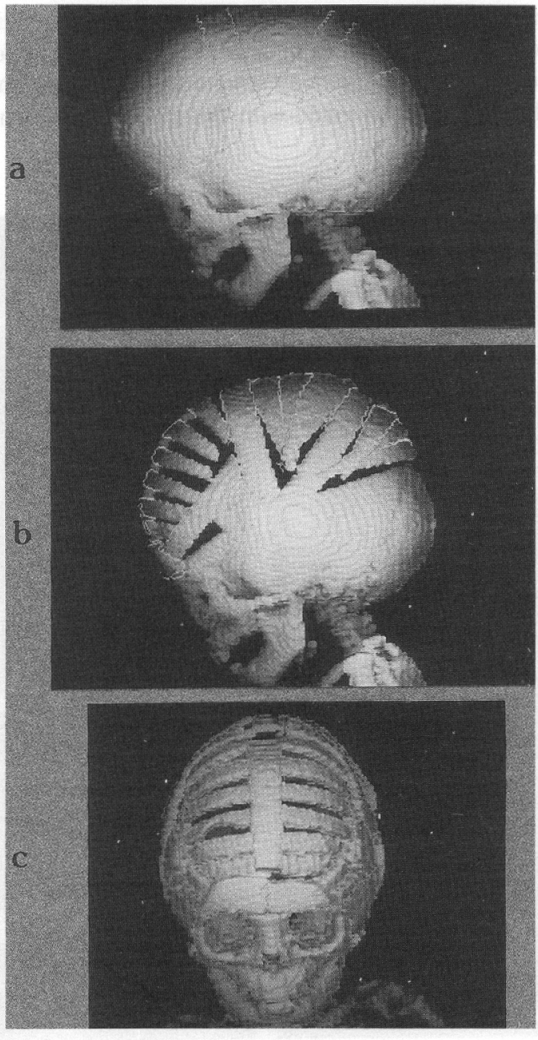

Fig. 9. Craniofacial surgical simulation. (a) Pre-operative skull with cut line, (b) Simulated skull (side view), (c) simulated skull (front view).

planes in object space. The cutting operations are assumed to divide an object by sweeping a closed 2-D contour on CT images (Herman, 1983; Brewster *et al.*, 1984; Trivedi, 1986). Fellingham *et al.* (1986) has developed a 3-D processing device with these functions called *CEMAX-1000*, and used for many clinical cases on business. It should be notified that available nanipulations are rather simple so that many actual manipulation for complex surgeries cannot be specified. An improved surgical simulation system to be used in actual clinical situation have been developed recently (Yasuda *et al.*, 1987, 1985, 1988). The idea here is to combine manipulative operations from several viewing directions in order to specify more complex osteotomies in actual surgeries. Prediction of soft-tissue alterations as a result of altering bony structures is also available. Craionfacial surgical simulation a surgeon made with this system is shown in Fig. 9. This

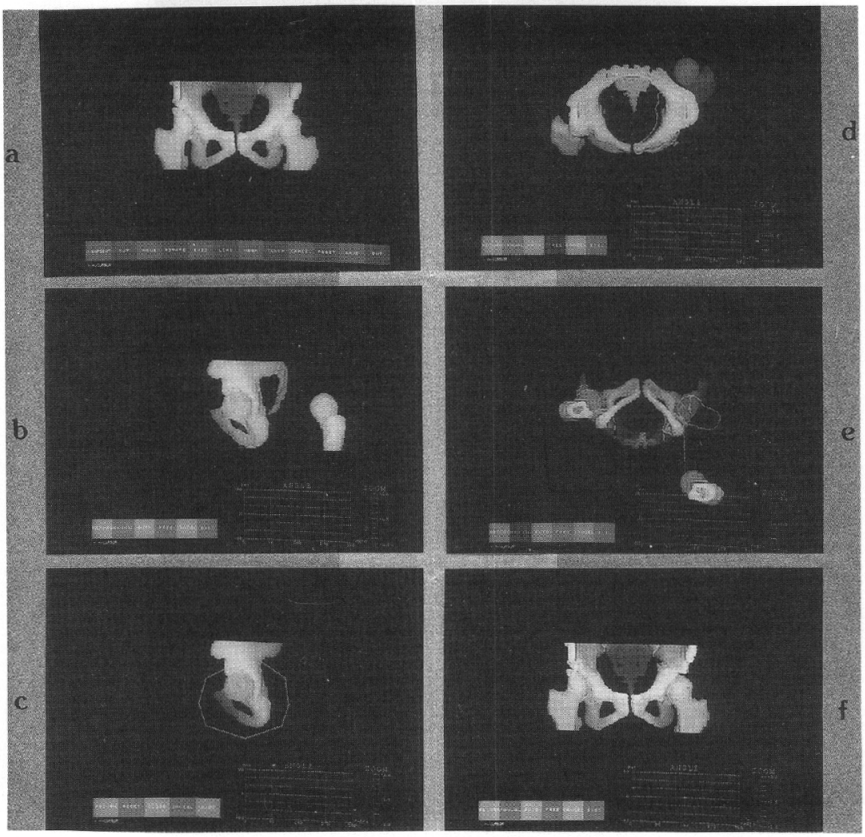

Fig. 10. Orthopaedic surgical simulation. (a) pre-operative image, (b) move left femur backward, (c) cut left pelvis, (d) rotate left pelvis, (e) set back left femur. (f) simulated image.

general approach has begun to be used for orthopaedic surgeries (Soyama *et al.*, 1989), and even for ancient mummy analysis (Yokoi *et al.*, 1989). They are shown in Fig. 10 and Fig. 11, respectively. Interactive manipulative techniques to alter an object from view space has a great deal of potential for simulating osteotomy in surgeries. Recently, several other researches for this purpose have been

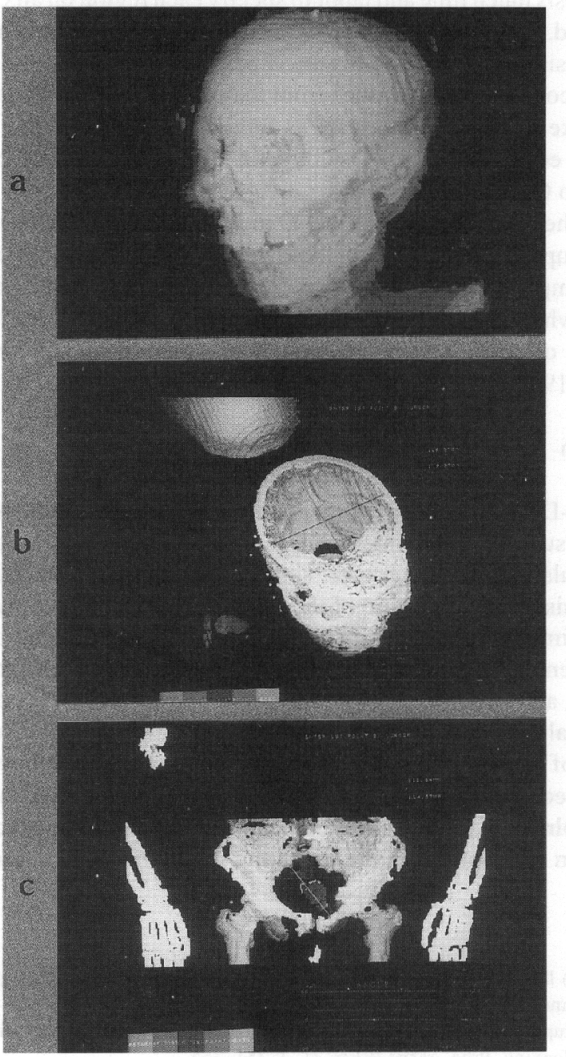

Fig. 11. Ancient Egyptian mummy analysis. (a) mummy face and skull, (b) analysis of the skull, (c) analysis of the pelvis.

reported (Ishii *et al.*, 1989; Suto *et al.*, 1989).

5.4 Automatic segmentation of adjacent bony regions

A reconstructed bony region is sometimes inseparable from its adjacent region due to partial volume effect of CT images. In orthopaedic surgical planning, it is necessary that pelvis and femur should be manipulated separately. While, in such cases, manual segmentation is the only way to overcome the problem, it costs much time and labor to specify each region on all CT images. On the other hand, it is possible to separate each of them automatically using 3-D image processing techniques (Soyama *et al.*, 1989). Advantages of 3-D image processings, compared to 2-D ones from the point of view of segmentation of a 3-D image like a set of CT slices are as follows.

(1) For edge detection, 3-D subtraction filter is able to detect edges which run parallel to CT slices.

(2) In the labeling process, by 2-D processing, different labels are given to voxels on the upper slice and one on the lower slice, although they consist the same connected component. On the other hand, 3-D process deals with them as the same component, when they are connected three dimensionally. Recently, automatic segmentation of pelvis and femur have been reported by another group (Ylä-Jääski *et al.*, 1988).

6. Conclusion

Using 3-D medical image processings and computer graphics, it is now possible to visualize human internal organs in three dimensions, and to interactively manipulate them on a graphic screen just as a surgeon would do during a surgery. In this article, the state of the art of visualization and manipulation of medical 3-D images have been surveyed. Examining the current developments, more improvement of image quality should be required from the point of view of visualization, and user friendly interface and high speed will be dispensable for routine clinical application. Since surgical planning is one of the most promising applications of medical 3-D imaging, more sophisticated techniques are expected to be developed in near future. For example, computer design of custom femoral stem (Granholm *et al.*, 1987; Kuno *et al.*, 1988) or simulating precise soft tissue reconstruction with analyzing the stress and/or strain are quite useful.

REFERENCES

Artzy, E. (1979) Display of three-dimensional information in computed tomography, Computer Graphics and Image Processing, 9, 196–198.

Bloch, P. and Udupa, J. K. (1983) Application of computerized tomography to radiation therapy and surgical planning, Proc. of the IEEE, 71, 3, 351–355.

Brewster, L. J., Trivedi, S. S., Tuy, H. K. and Udupa, J. K. (1984) Interactive surgical planning, IEEE Computer Graphics & Applications, 4, 31–40.

Chen, L. S., Herman, G. T., Reynolds, R. A. and Udupa, J. K. (1986) Surface shading in the cuberille environment, IEEE Computer Graphics & Applications, 5, 12, 33–43.

Christiansen, H. N. and Sederberg, T. W. (1978) Conversion of complex contour line definitions into polygonal element mosaics, Computer Graphics, 12, 187–192.

Drebin, R. A., Carpenter, L. and Hanrahan, P. (1988) Volume rendering, Computer Graphics, 22, 65–74.

Foley, J. D. and Dam. A. (1982) Fundamentals of interactive computer graphics, Addison-Wesley.

Fellingham, L. L., Vogel, J., Lau, C. and Dev, P. (1986) Interactive graphics and 3-D modeling for surgical planning and prosthesis and implant design, Proc. NCGA Computer Graphics, 132–142.

Frieder, G., Gordon, D. and Reynolds, R. A. (1985) Back-to-front display of voxel-based objects, IEEE Computer Graphics & Applications, 5, 1, 52–60.

Fuchs, H., Kedem, Z. M. and Uselton, S. P. (1977) Optimal surface reconstruction from planner contours, C.ACM, 20, 10, 693–702.

Gordon, D. and Reynolds, R. A. (1985) Image space shading of 3-dimensional objects, Computer Graphics and Imge Processing, 29, 3, 361–376.

Granholm, J. W., Robertson, D. D., Walker, P. S. and Nelson, P. C. (1987) Computer design of custom femoral stem protheses, IEEE Computer Graphics & Application, 7, 2, 26–35.

Herman, G. T. and Liu, H. K. (1979) Three-dimensional display of human organs from computed tomograms, Computer Graphics and Image Processing, 9, 1–21.

Herman, G. T. and Udupa, J. K. (1981) Display of 3D discrete surfaces, Proc. SPIE, 283, 90–97.

Herman, G. T. and Udupa, J. K. (1983) Display of 3-D digital images—Computational foundations and medical applications, 3, 5, 39–46.

Höhne, K. H. and Bernstein, R. (1986) Shading 3D-images from CT using gray-level gradients, IEEE Trans. Medical Imaging, 5, 1, 45–47.

Ishii, S. and Watanabe, E. (1989) Application of three-dimensional image to neorosurgery, Medical Imaging Technology, 7, 1, 9–15 (in Japanese).

Kaneda, Y., Fujii, S., Matsuo, M., Yoshida, M. and Kobashiri, Y. (1981) Automated pattern extraction and three-dimensional construction, Japanese Journal of Medical Electronics and Biological Engineering, 19, 4, 265–270 (in Japanese).

Keppel, E. (1975) Approximating complex surfaces by triangulation of contour lines, IBM Journal of Research and Development, 19, 2–11.

Kuno, T., Yokoi, S., Toriwaki, J. and Yasuba, S. (1988) Manufacturing artificial bone model using CT image data, IEICE Technical Report, IE87-117 (in Japanese).

Kurihara, T., Nakajima, H., Kaneko, T. *et al.* (1989) Surgical simulation with 3-D CT, Proc. of the 32nd. Annual Meeting of Japan Society of Plastic and Reconstructive Surgery.

Lin, W., Liang, C. and Chen, C. (1988) Dynamic elastic interpolation for 3-D medical sections, IEEE Trans. Medical Imaging, 7, 3, 225–232.

Lorensen, W. E. and Cline, H. E. (1987) Marching cubes: A high resolution 3D surface construction algorithm, Computer Graphics, 21, 163–168.

Ogino, Y., Kurata, K. and Makino, K. (1983) Textbook of plastic and reconstructive surgery (Nanzando company, Ltd. Tokyo).

Phong, B. T. (1984) Illumination for computer generated images, Computer Graphics, 18, 253–260.

Sutherland, I. E., Sproull, R. F. and Schumacker, R. A. (1974) A characterization of ten hidden-surface algorithms, Computing Surveys, 6, 1, 1–55.

Soyama, Y., Yasuda, T., Yokoi, S., Toriwaki, J., Izumida, R. and Fujioka, M. (1989) A hip joint surgical planning system using 3-D images, Japanese Journal of Medical Electronics and Biological Engeineering, 27, 2, 70–78 (in Japanese).

Suto, Y., Furuhata, K., Kojima, T., Kurokawa, T. and Kobayashi, M. (1989) Bone drilling simulation by three-dimensional imaging, Japanese Journal of Medical Electronics and Biological Engineering, 27, 2, 61–69 (in Japanese).

Toriwaki, J. (1986) Fundamental methods of recent three-dimensional display for medical images, Japanese Journal of Medical Electronies and Biological Engineering, 24, 5, 293–303 (in Japanese).

Trivedi, S. S. (1985) Representation of three-dimensional binary scenes, Proc. NCGA Computer Graphics, 132–144.

Trivedi, S. S. (1986) Interactive manipulation of three dimensional binary scenes, The Visual Computer, 2, 209–218.

Udupa, J. K. (1988) Computer graphics in surgical planning, Proc. NCGA Computer Graphics, 67–77.

Vannier, M. W., Marsh, J. L. and Warren, J. O. (1983) Three-dimensional computer graphics for craniofacial surgical planning and evaluation, Computer Graphics, 17, 263–273.

Yasuda, T., Toriwaki, J., Yokoi, S. and Katada, K. (1984) A three-dimensional display system of CT images for surgical planning, Proc. IEEE ISMII, 322–328.

Yasuda, T., Yokoi, S., Toriwaki, J., Fujioka, M. and Nakajima, H. (1985) Application of 3-D brain CT image display for craniofacial operation planning, Proc. NICOGRAPH, 189–196 (in Japanese).

Yasuda, T., Yorozu, J., Yokoi, S., Toriwaki, J. and Katada, K. (1986) Application of 3-D display of brain CT images to operation planning, Japnaese Journal of Medical Electronics and Biological Engineering, 24, 1, 22–27 (in Japanese).

Yasuda, T., Hashimoto, Y., Yokoi, S. and Toriwaki, J. (1987) Planning support system for craniofacial surgery using CT images, Trans. of the Institute of Electronics, Information and Communication Engineering, J70-D, 11, 2134–2140 (in Japnanese).

Yasuda, T., Hishimoto, Y., Goto, Y., Yokoi, S. and Toriwaki, J. (1988) Expansion of functions in a craniofacial surgical planning system using CT images, IEICE Technical Report, PRU88-8 (in Japanese).

Yasuda, T. (1989) Fundamental algorithms for medical 3-D image processings, IEICE Technical Report, PRU89-82 (in Japanese).

Yasuda, T., Hashimoto, Y., Yokoi, S. and Toriwaki, J. (1990) Computer system for craniofacial surgical planning based on CT images, IEEE Trans. Medical Imaging (in printing)

Ylä-Jääski, J. and Kubler, O. (1988) Segmentation and analysis of 3D volume images, IEEE 9th. Int. Conf. on Pattern Recogn., 951–953.

Yokoi, S., Toriwaki, J. and Fukumura, T. (1982) Survey of three-dimensional display for x-ray CT images. The society of Information Processing technical Report, CV18-5 (in Japanese).

Yokoi, S., Yasuda, T., Hashimoto, Y., Fujioka, M., Nakajima, H. and Toriwaki, J. (1987) A craniofacial surgical planning system, Proc. NCGA Computer Graphics, 152–161.

Yokoi, S., Ohshita, H., Yasuda, T. and Toriwaki, J. (1989) Three dimensional visualization and image analysis of an ancient Egyptian mummy, Proc. NICOGRAPH, 309–316 (in Japanese).